International Conference on Mathematics, Computational Methods & Reactor Physics (M&C 2009)
Saratoga Springs, New York, May 3-7, 2009, on CD-ROM, American Nuclear Society, LaGrange Park, IL (2009)

THE APPEARANCE OF COMPLEX VALUES IN MONTE CARLO CALCULATION OF DEGENERATE EIGENVALUES

Brian R. Nease
Commissariat á l'Énergie Atomique (CEA)
Saclay, France
bnease@gmail.com

Taro Ueki
Department of Chemical and Nuclear Engineering
University of New Mexico
Albuquerque, NM
tueki@unm.edu

ABSTRACT

The time series based Coarse Mesh Projection Method (CMPM) can be used to calculate both the fundamental and non-fundamental mode k-eigenvalues from a single run of iterated source Monte Carlo (MC) calculations. However, complex-valued intermediate eigensolutions are occasionally encountered in cases where the non-fundamental mode k-eigenvalues are degenerate or near-degenerate, even when the true eigenvalues are known to be real. For CMPM to be implemented and used in major production codes such as MCNP, Tripoli, etc., this discrepancy must be addressed. In this paper, the complex components are investigated and ways to properly eliminate them are provided.

Key Words: Monte Carlo, CMPM, criticality, complex eigenvalue

1. INTRODUCTION

Recently a technique termed the Coarse Mesh Projection Method (CMPM) was developed to calculate the k-eigenvalues of the fission source distribution in Monte Carlo (MC) calculations [1,2]. The method begins by applying an automatically determined projection vector to the discretized fission source distribution in stationarity, which transforms the process into a one-dimensional autoregressive process of order one (AR(1)). By applying time series techniques, the autocorrelation coefficient of the AR(1) process can be determined. This coefficient corresponds to the ratio of the desired mode k-eigenvalue to the fundamental mode k-eigenvalue (k_i/k_0, $i \geq 1$, and $|k_i| < |k_0|$). The method is very accurate given a sufficient number of active cycles and an appropriate fission source tally mesh.

CMPM automatically determines the projection vector from the eigenvectors of the Noise Propagation (NP) matrix $\mathbf{A}_0$, since these eigenvectors correspond to the eigenvalue ratios (k_i/k_0). The exact process will be detailed further in the next section. However, it will also be shown that the $\mathbf{A}_0$ matrix is not symmetric and can yield complex conjugate eigensolutions even

in problems where the true k-eigenvalues are proven to be real and in discrete spectrum (such as with mono-energetic transport in a finite geometry [3]). This is a potentially troubling aspect about the method that will be addressed in this paper.

Complex conjugate eigensolutions can appear in problems that have the multiplicity (degeneracy) of an eigenvalue due to geometric-material symmetry (such that multiple eigenmodes correspond to the same eigenvalue) or when two successive eigenvalues λ_i and λ_{i+1} are statistically indistinguishable, but not necessarily equal theoretically. For example, if $|\lambda_i - \lambda_{i+1}| < \sqrt{\text{var}[\lambda_i]}$ is obtained from one run of MC calculation, other runs might produce complex conjugates for λ_i and λ_{i+1}. When the eigenvalues are theoretically equal, it is not sufficient to simply run the problem with more neutrons or cycles (batches). If the eigenvalues are not theoretically equal, then it is possible to remove complex conjugate components by using more cycles. This might not always be practical, though, depending on how close the eigenvalues are. For this reason, an alternate method is presented that assures that real eigenvalue ratios are always obtained. As long as the true k-eigenvalues are real, this method will provide correct results.

The paper begins with a brief introduction to CMPM and how complex projection vectors are obtained. These components are then examined in an effort to explain their appearance and to quantify them. Finally, the method to account for the complex conjugate components is presented, followed by numerical results.

2. COARSE MESH PROJECTION METHOD (CMPM)

It has been shown [5] that the fluctuating part of the fission source distribution for the cycle $m+1$ in stationarity in an MC iterated source calculation can be represented in the form of a first order vector autoregressive process as

$$\vec{e}^{(m+1)} = \mathbf{A}_0 \vec{e}^{(m)} + \vec{\varepsilon}^{(m+1)} \tag{1}$$

where $\mathbf{A}_0$ is a $n \times n$ matrix termed the Noise Propagation (NP) matrix, $\vec{\varepsilon}^{(m+1)}$ is a random noise matrix of size $n \times 1$ for cycle $m+1$, and n is the number of spatial bins where the source distribution is tallied. It has also been shown [5] that the eigenvalues of $\mathbf{A}_0$ satisfy, in the original continuous space representation,

$$\left[\mathbf{A}_0 S_0\right](\vec{r}) = 0, \tag{2}$$

$$\left[\mathbf{A}_0 S_j\right](\vec{r}) = \frac{k_j}{k_0} S_j(\vec{r}) \qquad \text{if} \quad \int_V S_j(\vec{r})\, dV = 0,\ j \geq 1 \tag{3}$$

$$\begin{aligned} \left[\mathbf{A}_0 S_j\right](\vec{r}) &= \mathbf{A}_0 \left[S_j(\vec{r}) - S_0(\vec{r})\right] \\ &= \frac{k_j}{k_0}\left[S_j(\vec{r}) - S_0(\vec{r})\right] \quad \text{if} \quad \int_V S_j(\vec{r})\, dV \neq 0,\ j \geq 1 \end{aligned} \tag{4}$$

where $S_0(\vec{r})$ is the fundamental mode eigenfunction that corresponds to the fission source distribution with the eigenvalue k_0 (k_{eff}; effective multiplication factor), and $S_j(\vec{r}),\ j \geq 1$ are

the non-fundamental mode eigenfunctions that correspond to the eigenvalues k_j, $j \geq 1$, $|k_j| < |k_0|$. Thus, the eigenvalues of the NP matrix correspond to the ratio of the non-fundamental mode k-eigenvalues to the fundamental mode k-eigenvalue in the original criticality problem. CMPM was developed to estimate the NP matrix and extract these eigenvalue ratios via time series techniques. To ensure that the directions for projecting the fluctuating part $\vec{e}^{(m)}$ were all linearly independent, the eigenvalue problem that we consider is that of the transpose of the $\mathbf{A}_0$ matrix:

$$\mathbf{A}_0^{\mathbf{T}} \vec{p}_i = \lambda_i \vec{p}_i \tag{5}$$

where $\mathbf{T}$ signifies the transpose and λ_i corresponds to the eigenvalue ratio k_i/k_0 $\left(\lambda_i \cong k_i/k_0\right)$. The process of CMPM is to 1) estimate the linearly independent eigenvectors of $\mathbf{A}_0^{\mathbf{T}}$, 2) project the source fluctuation $\vec{e}^{(m)}$ onto the desired eigenvector, and 3) solve for the corresponding eigenvalue ratio from a time series of $\vec{p}_i^{\,T}\vec{e}^{(m)}$. However, as will be shown later, the NP matrix is not symmetric, which can lead to potential problems when calculating the eigenvectors in step 1). Specifically, the eigenvectors of a non-symmetric matrix are not guaranteed to be real. Even when analyzing problems that are known to have real eigensolutions, there is a chance that some estimate of $\mathbf{A}_0^{\mathbf{T}}$ may have complex eigenvectors due to the statistical fluctuations inherent to MC.

The matrix form of $\mathbf{A}_0^{\mathbf{T}}$ used in step 1) will be derived first. Multiplying both sides of Eq. (1) by $\left(\vec{e}^{(m)}\right)^{\mathbf{T}}$ from the right and taking the expectation yields

$$E\left[\vec{e}^{(m+1)}\left(\vec{e}^{(m)}\right)^{\mathbf{T}}\right] = \mathbf{A}_0 E\left[\vec{e}^{(m)}\left(\vec{e}^{(m)}\right)^{\mathbf{T}}\right] \tag{6}$$

since [1]

$$E\left[\vec{\varepsilon}^{(m+1)}\left(\vec{e}^{(m)}\right)^{\mathbf{T}}\right] = 0\,. \tag{7}$$

New notations are introduced for later discussion:

$$\mathbf{L}_1 = \mathbf{A}_0 \mathbf{L}_0 \tag{8}$$

where

$$\mathbf{L}_j = E\left[\vec{e}^{(m+j)}\left(\vec{e}^{(m)}\right)^{\mathbf{T}}\right] \tag{9}$$

Solving for $\mathbf{A}_0$ gives the product of two lag cross covariance matrices

$$\mathbf{A}_0 = \mathbf{L}_1 \mathbf{L}_0^{-1}\,. \tag{10}$$

Since the matrix $\mathbf{L}_1$ is not symmetric, the solution of an estimate of $\mathbf{A}_0$ may yield complex eigensolutions due to statistical fluctuations, even for problems known to have real solutions. However, since it is a real matrix, the complex eigensolutions always appear as complex conjugate pairs. The eigenvector $\vec{p}_i$ of the estimated transpose matrix $\mathbf{A}_0^{\mathbf{T}}$ corresponding to the desired eigenvalue $\lambda_i = k_i / k_0$ is chosen as the projection vector to ensure that the directions for projection are linearly independent and will not influence each other [6]. Accounting for the possibility of complex eigenvectors through complex time series techniques, it has been shown based on time series analysis [6] that the eigenvalue ratio can be solved for as

$$\frac{k_i}{k_0} \cong \lambda_i = \frac{\vec{p}_i^{\mathbf{T}} \mathbf{L}_1 \vec{p}_i^{*}}{\vec{p}_i^{\mathbf{T}} \mathbf{L}_0 \vec{p}_i^{*}}. \tag{11}$$

where $\vec{p}_i = \vec{p}_i^{R} + i\vec{p}_i^{I}$ and the complex conjugate is $\vec{p}_i^{*} = \vec{p}_i^{R} - i\vec{p}_i^{I}$.

Interestingly, it can be shown that the equality in Eq (11) can be derived in a different manner. Starting from Eq (5), we consider that

$$\vec{p}_i^{\mathbf{T}} \mathbf{A}_0 = \lambda_i \vec{p}_i^{\mathbf{T}}. \tag{12}$$

Applying Eq (10) yields

$$\vec{p}_i^{\mathbf{T}} \mathbf{L}_1 \mathbf{L}_0^{-1} = \lambda_i \vec{p}_i^{\mathbf{T}} \tag{13}$$

or

$$\vec{p}_i^{\mathbf{T}} \mathbf{L}_1 = \lambda_i \vec{p}_i^{\mathbf{T}} \mathbf{L}_0. \tag{14}$$

Multiplying Eq (14) on the right by $\vec{p}_i^{*}$ results in

$$\vec{p}_i^{\mathbf{T}} \mathbf{L}_1 \vec{p}_i^{*} = \lambda_i \vec{p}_i^{\mathbf{T}} \mathbf{L}_0 \vec{p}_i^{*} \tag{15}$$

which is equivalent to Eq (11). This has three important implications. First, the equality in Eqs (11) and (15) is general in the sense that it holds irrespective of the expressions of $\mathbf{L}_0$ and $\mathbf{L}_1$ if $\mathbf{A}_0$ in the eigenvalue problem in Eqs (5) and (12) is equal to $\mathbf{L}_1 \mathbf{L}_0^{-1}$. Second, the first order vector autoregressive representation allows one to compute $\vec{p}_i^{\mathbf{T}} \mathbf{L}_0 \vec{p}_i^{*}$ and $\vec{p}_i^{\mathbf{T}} \mathbf{L}_1 \vec{p}_i^{*}$ via projection and time series [6], though the projection and time series process does not provide any gain in information mathematically; it may be sufficient to simply solve $\mathbf{A}_0$. However, if the desired eigenvalues are statistically indistinguishable, they could be estimated as complex conjugate eigenvalues even in cases where the solutions are known to be real. These solutions would be neither practical nor correct and could be misleading to code users. For this reason, the complex eigenvalues and eigenvectors of $\mathbf{A}_0^{\mathbf{T}}$ should not be used. Instead, an assumption is made that all results are real, and that the two necessarily linearly independent real vectors can be approximated by the individual real and imaginary parts of the complex eigenvector. The argument for using these individual parts of the eigenvector is discussed in the next section. Third, perhaps most important practically, the time series analysis provides the capability of calculating the standard deviation of $\lambda_i = k_i / k_0$ from a single run of an iterated source MC calculation [6] as presented in the next section by Eq (27).

3. ACCOUNTING FOR COMPLEX CONJUGATE EIGENSOLUTIONS

For an eigenmode with a multiplicity of two, there exists two linearly independent eigenvectors of $\mathbf{A}_0^{\mathbf{T}}$ that share the same eigenvalue λ. These two eigenvectors form a linear subspace of $\mathbf{A}_0^{\mathbf{T}}$ called an eigenspace, which has a dimension of two. Although CMPM sometimes produces complex conjugate eigenvectors that correspond to λ, we should always be able to find two linearly independent eigenvector estimates in the real domain to apply as a projection vector. In this section we assert that the real and imaginary part of the complex conjugate estimates of the eigenvectors, denoted as $\vec{p}_R$ and $\vec{p}_I$, can each, individually be used as a good approximation to these two linearly independent real eigenvectors. The argument for this assertion follows by

first proving that the two vectors $\vec{p}_R$ and $\vec{p}_I$ are indeed linearly independent. Afterwards, we show that using these two vectors as approximations to the eigenvalue problem in Eq (5) results in a real eigenvalue approximation, provided that the magnitude of the imaginary component of λ is small compared to that of the real component. In this way, two real eigenvalue approximations can always be obtained when complex conjugate eigensolutions appear due to multiplicity in the problem.

To prove that the two eigenvectors $\vec{p}_R$ and $\vec{p}_I$ are linearly independent, we first define the complex conjugate eigenvalue problem as

$$\begin{aligned} \mathbf{A}_0^{\mathbf{T}}\left(\vec{p}_R + i\vec{p}_I\right) &= \left(\lambda_R + i\lambda_I\right)\left(\vec{p}_R + i\vec{p}_I\right) \\ \mathbf{A}_0^{\mathbf{T}}\left(\vec{p}_R - i\vec{p}_I\right) &= \left(\lambda_R - i\lambda_I\right)\left(\vec{p}_R - i\vec{p}_I\right) \end{aligned}. \tag{16}$$

such that $\vec{p}_R$ and $\vec{p}_I$ are real vectors, λ_R and λ_I are real numbers and *i* is the imaginary unit $\left(i^2 = -1\right)$. If we consider that the real vectors $\vec{p}_R$ and $\vec{p}_I$ are linearly dependent, i.e.,

$$\vec{p}_I = C\vec{p}_R . \tag{17}$$

then the eigenvalue equation becomes

$$\begin{aligned} \left(1+iC\right)\mathbf{A}_0^T\vec{p}_R &= \left(\lambda_R + i\lambda_I\right)\left(1+iC\right)\vec{p}_R \\ \left(1-iC\right)\mathbf{A}_0^T\vec{p}_R &= \left(\lambda_R - i\lambda_I\right)\left(1-iC\right)\vec{p}_R \end{aligned} \tag{18}$$

or

$$\begin{aligned} \mathbf{A}_0^T\vec{p}_R &= \left(\lambda_R + i\lambda_I\right)\vec{p}_R \\ \mathbf{A}_0^T\vec{p}_R &= \left(\lambda_R - i\lambda_I\right)\vec{p}_R \end{aligned}. \tag{19}$$

Subtract these two equations to obtain

$$0 = i\lambda_I\vec{p}_R . \tag{20}$$

Therefore, $\lambda_I = 0$. By contraposition, if $\lambda_I \neq 0$, then $\vec{p}_R$ and $\vec{p}_I$ must be linearly independent.

Next, we show that $\vec{p}_R$ and $\vec{p}_I$ each, individually provide good approximations to the actual eigenvectors, provided that $|\lambda_I| \ll |\lambda_R|$. Taking the sum of the two equations in Eq (16) yields

$$\mathbf{A}_0^{\mathbf{T}}\left(\vec{p}_R + i\vec{p}_I + \vec{p}_R - i\vec{p}_I\right) = \left(\lambda_R + i\lambda_I\right)\left(\vec{p}_R + i\vec{p}_I\right) + \left(\lambda_R - i\lambda_I\right)\left(\vec{p}_R - i\vec{p}_I\right) \tag{21}$$

$$\mathbf{A}_0^{\mathbf{T}}\left(2\vec{p}_R\right) = 2\lambda_R\vec{p}_R - 2\lambda_I\vec{p}_I . \tag{22}$$

Assuming that $|\lambda_I| \ll |\lambda_R|$, then we can make the approximation that Eq (22) becomes

$$\mathbf{A}_0^{\mathbf{T}}\vec{p}_R = \lambda_R\vec{p}_R - \lambda_I\vec{p}_I \approx \lambda_R\vec{p}_R . \tag{23}$$

Similarly, subtracting the two equations in (16) yields

$$\mathbf{A}_0^{\mathbf{T}}\left(\vec{p}_R + i\vec{p}_I - \vec{p}_R + i\vec{p}_I\right) = \left(\lambda_R + i\lambda_I\right)\left(\vec{p}_R + i\vec{p}_I\right) - \left(\lambda_R - i\lambda_I\right)\left(\vec{p}_R - i\vec{p}_I\right) \tag{24}$$

$$\mathbf{A}_0^{\mathbf{T}}\left(2i\vec{p}_I\right) = 2i\lambda_R\vec{p}_I + 2i\lambda_I\vec{p}_R . \tag{25}$$

Again, assuming that $|\lambda_I| \ll |\lambda_R|$ we can make the approximation that Eq (25) becomes

$$\mathbf{A}_0^{\mathbf{T}}\vec{p}_I = \lambda_R\vec{p}_I + \lambda_I\vec{p}_R \approx \lambda_R\vec{p}_I . \tag{26}$$

Thus, both linearly independent vectors $\vec{p}_R$ and $\vec{p}_I$ provide a good approximation to the two distinct real eigenvectors if $0 < |\lambda_I| \ll |\lambda_R|$. This method is very easy to implement and the solutions are practical since the solutions are guaranteed to be real.

Lastly, the error of a real estimate of AR(1) autocorrelation coefficient, which in our case is equal to the desired eigenvalue ratio $\lambda_i = k_i / k_0$ [6], is [7]

$$\sqrt{\text{var}[\lambda_i]} = \sqrt{\frac{1}{M}(1-\lambda_i^2)} \tag{27}$$

where *M* is the number of active cycles. This formula can be used to compute the standard deviation from a single run of an iterated source MC calculation.

4. PROBLEM DESCRIPTIONS

There are two problems that were repeatedly tested in the following result section:

Problem 1 is a monoenergetic two-dimensional checkerboard problem with vacuum boundary conditions shown in Figure 1. There are two types of fuel placed alternately in a checkerboard manner making the problem symmetric along the diagonals. There exists multiplicity such that the first two non-fundamental mode k-eigenvalues are theoretically equal. The eigenvalue ratio k_1/k_0, termed the dominance ratio (DR), was estimated to be 0.9581 by the analysis of the spectral radius of the outer iterations in discontinuous finite element discrete ordinates methods [8]. The effective neutron multiplication factor was calculated to be 1.05450 by the discrete ordinates method and 1.054504 ± 0.000010 by MC.

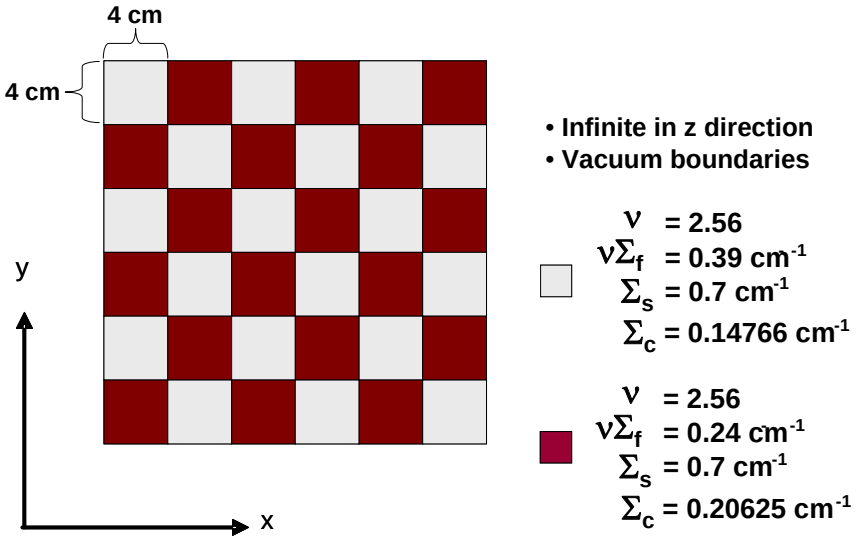

Figure 1: Makeup of 1-D inhomogeneous slab problem

Problem 2 is a monoenergetic one-dimensional multi-material-region slab with vacuum boundary conditions shown in Figure 2. There are two fuel (fissile) regions on either side of the slab with scattering and absorbing material between them. This type of problem would most likely be found in criticality safety work. The $\lambda_2 = k_2/k_0$ eigenvalue ratio and the $\lambda_3 = k_3/k_0$

eigenvalue ratio were calculated to be 0.304653 and 0.304635, respectively, by the Green's Function Method (GFM) [9] with a 1,800 bin mesh across the entire problem domain. While not exactly equal, these eigenvalue ratios are close enough to be statistically indistinguishable unless an unreasonably large number of active cycles are used. The effective neutron multiplication factor was calculated to be 0.424314 by GFM and 0.424314 ± 0.000007 by MC.

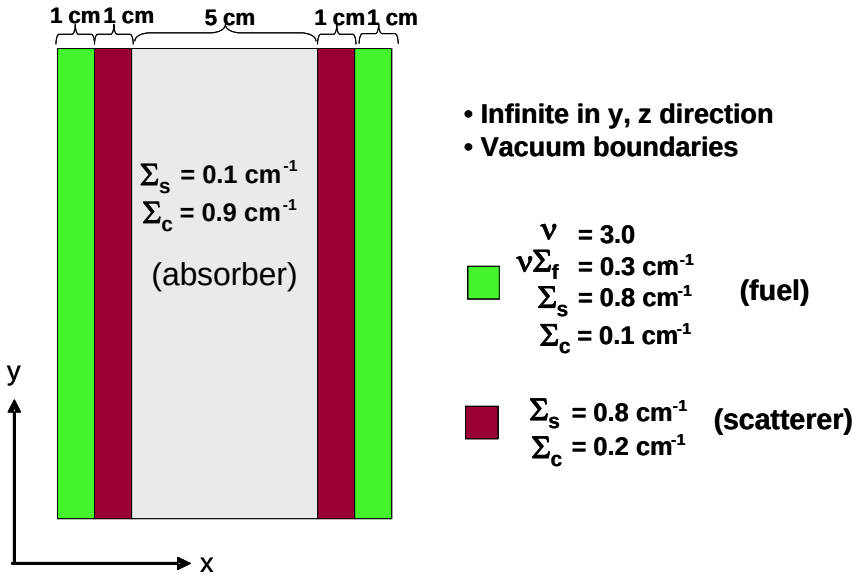

Figure 2: Makeup of 1-D inhomogeneous slab problem

5. RESULTS

The frequency of obtaining complex conjugate eigensolutions roughly varied between 20% - 30%. For example, 300 runs of Problem 1 were made using 10,000 particles per cycle and 10,000 active cycles. The frequency of complex conjugate estimates of the λ_1 and λ_2 eigenvalues of $\mathbf{A}_0$ was 33%. 50 runs of Problem 2 were also made using 30,000 particles per cycle and 11,000 active cycles. The frequency of complex conjugate eigensolutions in this case was 20%.

While in general the complex components never disappear when multiplicity exists, the magnitude of the complex parts of the eigenvalue compared to the magnitude of the real part does decrease as the number of active cycles increases. The 100 runs of Problem 1 that resulted in the complex k_1/k_0 eigensolutions of $\mathbf{A}_0$ were analyzed against varying numbers of active cycles. The DR (k_1/k_0) was calculated after every active cycle in each of the 100 runs and the average magnitude of the imaginary part was plotted in a log-log plot in Figure 3. This is contrasted against M^{-1} and $M^{-1/2}$ (where M is the number of active cycles) to illustrate how the imaginary part decreases. As can be seen, the magnitude is bounded and appears to decrease no slower than $M^{-1/2}$.

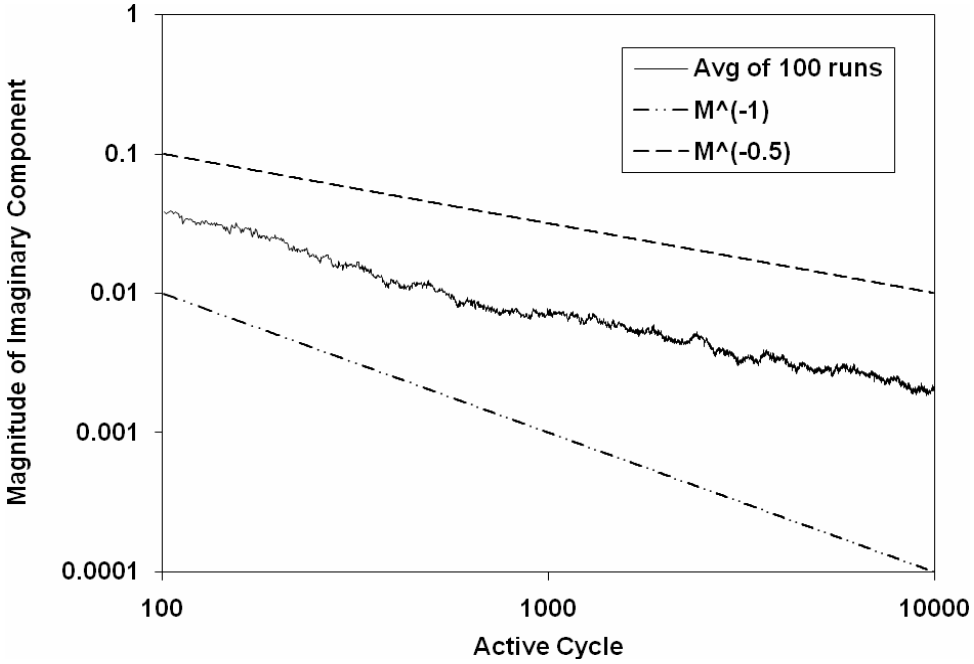

Figure 3: Magnitude of Imaginary Part of k1/k0 Eigenvalue of A_0 in Problem 1

The 300 independent runs of Problem 1 using 10,000 particles per cycle and 10,000 active cycles were analyzed again (calculating DR, i.e. k_1 / k_0) and the results are shown in Table 1 and Table 2. Out of the total 300 runs, the k_1 / k_0 eigenvalue of $\mathbf{A}_0^{\mathbf{T}}$ was calculated as a real quantity 200 times and as a complex quantity 100 times. In all cases, the standard deviation was calculated as the standard deviation of the mean, such that

$$\bar{\sigma}_\lambda = \left(\frac{1}{N(N-1)} \sum_{i=1}^{N} \left(\lambda_i - \bar{\lambda} \right)^2 \right)^{1/2}; \quad \bar{\lambda} = \frac{1}{N} \sum_{i=1}^{N} \lambda_i \tag{28}$$

where N is the number of independent runs. Table 1 compares three different calculations of the k_1 / k_0 eigenvalue: the benchmark discrete ordinates method result, the average CMPM eigenvalue over the 200 runs producing real eigenvectors for the largest eigenvalue of $\mathbf{A}_0^{\mathbf{T}}$, and the average eigenvalue of the $\mathbf{A}_0^{\mathbf{T}}$ matrix over the same 200 runs. Note the standard deviation in CMPM was not computed using Eq (27).

	Benchmark Discrete Ordinates	CMPM ± 2σ Using Real Part of Eigenvector	CMPM ± 2σ Using Imaginary Part of Eigenvector	Eigenvalue of Ao Matrix ± 2σ
k_1/k_0	0.9581	0.95833 ± 0.00036 (0.95797, 0.95869)	N / A	0.95833 ± 0.00036 (0.95797, 0.95869)

Table 1: k_1/k_0 of Problem 1 using CMPM with 4-bin mesh and 2σ std. dev. for runs with real intermediate results

As expected, the two results are the same up to five significant digits. Obviously, the imaginary part of the vector could not be used since it is zero (trivial) in this case. Table 2 compares four

different calculations of the k_1 / k_0 eigenvalue ratio: the benchmark discrete ordinates method result, the average CMPM eigenvalue over the 100 runs producing complex eigenvectors for the largest eigenvalue of $\mathbf{A}_0^{\mathbf{T}}$ and using solely the real part of the eigenvector or solely the imaginary part of the eigenvector, and the average eigenvalue of the $\mathbf{A}_0^{\mathbf{T}}$ matrix over the same 100 runs.

	Benchmark Discrete Ordinates	CMPM ± 2σ Using Real Part of Eigenvector	CMPM ± 2σ Using Imaginary Part of Eigenvector	Eigenvalue of Ao Matrix Real + Imaginary
k_1/k_0	0.9581	0.95566 ± 0.00041 (0.95525, 0.95607)	0.95563 ± 0.00044 (0.95519, 0.95607)	0.95547 + 0.00207i

Table 2: k_1/k_0 of Problem 1 using CMPM with 4-bin mesh and 2σ std. dev. for runs with complex intermediate results

The first observation that we make is that using solely the real or imaginary part of the eigenvector as the projection vector did not give significantly different results than just taking the real part of the eigenvalue of the $\mathbf{A}_0^{\mathbf{T}}$ matrix. Even in complex cases, it appears that the real part of the eigenvalue of the $\mathbf{A}_0^{\mathbf{T}}$ matrix can always be used as to approximate the desired eigenvalue ratio. The second observation is that, as expected, the eigenvalues obtained from using solely the real and imaginary parts of the $\mathbf{A}_0^{\mathbf{T}}$ eigenvector are statistically indistinguishable. The two error bounds overlap: (0.95525, 0.95607) for the real part and (0.95519, 0.95607) for the imaginary part. For the same 100 runs, we have performed higher order autoregressive fitting to see if the estimation of k_1 / k_0 improves or not. As seen in Table 3, the upper end of 2σ confidence interval from the fourth order fitting is equal to the benchmark discrete ordinates result through the four significant digits. The k_1 / k_0 eigenvalue ratio was also computed to be 0.95740 with the fission matrix method [10] using $2304 = 48 \times 48$ bins. The third and fourth order autoregressive fitting results contain this value within 1σ confidence interval.

	Benchmark Discrete Ordinates	CMPM ± 2σ Using Real Part of Eigenvector			
		AR fitting order			
		1	2	3	4
k_1/k_0	**0.9581**	0.95566±0.00041	0.95681±0.00045	0.95750±0.00048	0.95755±0.00054

Table 3: k_1/k_0 of Problem 1 Using higher order autoregressive fitting and CMPM with 4-bin Mesh for runs with complex intermediate results

One particular run of Problem 2 using 11,000 active cycles and 30,000 particles per cycle also resulted in the complex conjugate estimates of eigenvalues of $\mathbf{A}_0$ for k_2 / k_0 and k_3 / k_0 when using a 25-bin mesh across the two fuel regions. The eigenvalue ratios k_2 / k_0 and k_3 / k_0 were calculated using solely the real part $\vec{p}_R$ and then solely the imaginary part $\vec{p}_I$ of the eigenvector as the projection vector as explained before. The results are shown in Table 4 where the standard deviation (σ) in CMPM was computed using Eq (27). These were compared to a benchmark value that used the Green's Function Method with an 1,800 bin mesh across the problem domain. As can be seen, both estimates correctly contain the benchmark result. In passing, $k_2 = 0.129269$, $k_3 = 0.129262$ and $k_0 = 0.42316$ by Green's Function Method. There is no established method to compute the standard deviations of eigenvalue estimates for the raw

matrix solver solutions of $\mathbf{A}_0^{\mathbf{T}}$. Therefore, the fifth column does not exist in Table 4 unlike Table 2.

	GFM Using 1,800-Bin Mesh	CMPM 2σ CI Using Real Part of Eigenvector	CMPM 2σ CI Using Imaginary Part of Eigenvector
k_2/k_0, k_3/k_0	0.304653, 0.304636	(0.293625, 0.329863)	(0.288569, 0.324869)

Table 4: k_2/k_0 & k_3/k_0 of Problem 2 using real & imaginary part of eigenvector in CMPM with 25-bin mesh and 2-σ std. dev.

6. CONCLUSIONS

Complex estimates of intermediate eigensolutions are encountered roughly 20% - 30% of the time when applying CMPM to calculate eigenvalue ratios (k_i / k_0) that are statistically indistinguishable. While this can appear incorrect and misleading, it does yield insight into the nature of problem and its multiplicity. We have shown that by applying solely the real and imaginary parts of the complex estimate of $\mathbf{A}_0^{\mathbf{T}}$ eigenvector ($\mathbf{A}_0$; noise propagation matrix), real estimates of k_i / k_0 can be always guaranteed. In case of these complex estimates, there does appear to be a slight bias in the final estimate. However, this bias can be eliminated using higher order autoregressive fitting. It will be worthwhile to investigate 1) problems with a multiplicity of three, 2) varying source tally bin structure across the problem domain, and 3) characterization of the two dimensional trajectory of complex time series.

REFERENCES

[1] B.R. Nease & T. Ueki, "Time Series Analysis of Monte Carlo Fission Sources: III. Coarse Mesh Projection," Nuc. Sci. and Eng., 157, pp. 51-64, (2007).

[2] B.R. Nease and T. Ueki, "Higher Eigenmode Analysis with Coarse Mesh Projection in Monte Carlo Fission Source Iterations," *Transactions of American Nuclear Society* **98**, 515 (2008).

[3] D.C. Sahni, "Some New Results Pertaining to Criticality and Time Eigenvalues of One-Speed Neutron Transport Equation," Progress in Nuclear Energy, 30, 3, pp. 305-320, (1996).

[4] H. von Storch, et. al., "Principal Oscillation Patterns: A Review," Journal of Climate, 8, 3, pp. 377-400, (1995).

[5] T. Ueki, F.B. Brown, D.K. Parsons, and J.S. Warsa, "Time Series Analysis of Monte Carlo Fission Sources: I. Dominance Ratio Computation," Nuclear Science and Engineering, 148, 374-390, (2004).

[6] B.R. Nease, "Time Series Analysis of Monte Carlo Neutron Transport Calculations," Ph.D. dissertation, Dept. of Chem. and Nuclear Eng., University of New Mexico, (2008).

[7] G.E. Box, G.M. Jenkins & G.C. Reinsel, *Time Series Analysis: Forecasting and Control*, Prentice-Hall, Inc., Upper Saddle River, NJ 1997.

[8] Wareing T.A., McGhee J.M., Morel J.E., Pautz S.D. (2001). Discontinuous finite element Sn methods on three-dimensional unstructured grids, Nuc. Sci. and Eng., 138, p 256.

[9] Kornreich D.E., Parsons D.K. (2003). The Green's function method for effective multiplication benchmark calculations multi-region slab geometry, Ann. Nucl. Energy, **31**, 13 1477.

[10] Morton K.W. (1956). Criticality Calculations by Monte Carlo methods, AERE-TR-1903, Harwell.